CHEMMEDCHEM
Chemistry & Drug Discovery

Supporting Information

Small Molecule Binding to Proteins: Affinity and Binding/Unbinding Dynamics from Atomistic Simulations

Danzhi Huang* and Amedeo Caflisch*[a]

cmdc_201100237_sm_miscellaneous_information.pdf

Materials and Methods

MD simulations. The coordinates of FKBP were downloaded from the PDB database (entry 1D7H). To reproduce neutral pH conditions the side chains of aspartates and glutamates were negatively charged, those of lysines and arginines were positively charged, and histidines were considered neutral. The protein was immersed in an orthorhombic box of preequilibrated water molecules. The size of the box was chosen to have a minimal distance of 13 Å between the boundary and any atom of the protein. Twenty-five, 50, and 100 copies of dimethylsulfoxide (DMSO), corresponding to concentrations of 220, 440, and 880 mM, respectively, were placed randomly in the bulk water. Water molecules within 2.4 Å of any heavy atom of the protein or DMSO were removed except for six water molecules present in the crystal structure. The simulation system contained 8 sodium and 9 chloride ion to compensate for the total charge of FKBP which is +1 electron units. The MD simulations were carried out with NAMD [1] using the CHARMM22 force field [2] and the TIP3P model of water [3]. The parameters of DMSO were determined according to the general CHARMM force field [4]. The partial charges (in electronic units) of the DMSO sulfinyl oxygen and sulfur atoms are -0.556 and 0.312, respectively, while the partial charges of the methyl carbon and hydrogen atoms are -0.148 and 0.09, respectively.

Periodic boundary conditions were applied and electrostatic interactions were evaluated using the particle-mesh Ewald summation method [5]. The van der Waals interactions were truncated at a cutoff of 12 Å and a switch function was applied starting at 10 Å. The MD simulations were performed at constant temperature (310 K) using the Langevin thermostat and constant pressure (1 atm) [6] with a time step of 2 fs. The SHAKE algorithm was used to fix the covalent bonds involving hydrogen atoms.

Analysis of MD simulations and clustering procedure. The analysis of the MD trajectories was carried out with CHARMM [7] and the MD-analysis tool WORDOM [8]. The leader algorithm as implemented in the latter program was employed for clustering according to the distance root mean square between two MD snapshots a and b,

DRMS $= [n^{-1} \sum_{(i,j)}^{n} (d_{ij}^{\mathrm{a}} - d_{ij}^{\mathrm{b}})^2]^{1/2}$, which was calculated using the intermolecular distances d_{ij} between pairs of non-hydrogen atoms in DMSO and eight residues in the FKBP active site (Tyr26, Asp37, Phe46, Val55, Ile56, Trp59, Tyr82, and Phe99). A DRMS threshold of 1 Å was used for clustering by the leader algorithm. The DRMS calculation does not require structural overlap. In other words, rigid-body fitting is not necessary, which is an advantage with respect to the root mean square deviation.

Stability of FKBP in the MD simulations

The FKBP structure is stable during the simulation as indicated by the low RMSF values (blue color in Figure 1) despite the high DMSO concentration (0.44 M). Moreover, the C_α root mean square deviation from the X-ray structure is < 2 Å for 75% and > 3 Å for only 4% of the snapshots at 310 K. This result is also consistent with the fact that experimentally FKBP remains stable up to 1.5 M DMSO [9]. The most flexible part is the flap region (80's loop, red) which also agrees with previous observation of FKBP in solution using NMR spectroscopy [10]. In fact, the flexibility of the flap region of FKBP facilitates access of substrates and inhibitors to the enzyme active site [11]. The agreement between the simulation and experiment indicates that the force field and simulation protocol are adequate for investigating DMSO binding to and unbinding from FKBP.

References

[1] Phillips JC, Braun R, Wang W, Gumbart J, Tajkhorshid E, et al. (2005) Scalable molecular dynamics with namd. J Comput Chem 26: 1781–1802.

[2] MacKerell Jr ea AD, M K (1998) All-atom empirical potential for molecular modeling and dynamics studies of proteins. J Phys Chem B 102: 3586-3616.

[3] Jorgensen WL, Chandrasekhar J, Madura J, Impey RW, Klein ML (1983) Comparison of simple potential functions for simulating liquid water. J Chem Phys 79: 926-935.

[4] Vanommeslaeghe K, Hatcher E, Acharya C, Kundu S, Zhong S, et al. (2010) CHARMM general force field: A force field for drug-like molecules compatible with the CHARMM all-atom additive biological force fields. J Comput Chem 31: 671-690.

[5] Darden T, York D, Pedersen LG (1993) Particle mesh Ewald: an Nlog(N) method for Ewald sums in large systems. J Chem Phys 98: 10089.

[6] Feller S, Zhang Y, Pastor R, Brooks B (1995) Constant pressure molecular dynamics simulation: the Langevin piston method. jcp 103: 4613.

[7] Brooks BR, Brooks III CL, Mackerell ADJ, Nilsson L, Petrella RJ, et al. (2009) CHARMM: the biomolecular simulation program. J Comput Chem 30: 1545-614.

[8] Seeber M, Cecchini M, Rao F, Settanni G, Caflisch A (2007) Wordom: a program for efficient analysis of molecular dynamics simulations 23: 2625-2627.

[9] Dalvit C, Floersheim P, Zurini M, Widmer A (1999) Use of organic solvents and small molecules for locating binding sites on proteins in solution. Journal of Biomolecular NMR 14: 23–32.

[10] Cheng J, Lepre C, Moore J (1994) 15N NMR relaxation studies of the FK506 binding protein: dynamic effects of ligand binding and implications for calcineurin recognition. Biochemistry 33: 4093–4100.

[11] Park S, Aldape R, Futer O, DeCenzo M, Livingston D (1992) PPIase catalysis by human FK506-binding protein proceeds through a conformational twist mechanism. Journal of Biological Chemistry 267: 3316.

Robustness of binding/unbinding rates upon changes of binding/unbinding thresholds.

Binding; Unbinding thresholds (Å)	τ_{on} (ns)	τ_{off} (ns)	k_{off}/k_{on} [a] (mM)	K_D [b] (mM)
4; 8	2.6	4.1	279	**360**
5; 8	2.1	2.6	355	
4; 9	2.8	4.8	**256**	303
5; 9	2.5	3.5	314	

Table 1: [a]**Kinetic analysis.** Dissociation constant from fitting of cumulative distributions of unbinding and binding times. The characteristic time of the slow phase of the double-exponential fitting is used to calculate the binding rate $k_{on} = 1/(\tau_{on}[\text{DMSO}])$ and unbinding rate $k_{off} = 1/\tau_{off}$. The concentration of DMSO in the simulation box is 440 mM.
[b]**Thermodynamic analysis.** Dissociation constant calculated from active site occupancy K_D = [DMSO] [unbound FKBP] / [bound FKBP] = 440 mM $\times$ 0.45/0.55 = 360 mM. Note that the concentration of DMSO does not change significantly upon binding because of the DMSO:FKBP ratio of 50:1 in the simulation box. The active site occupancy was determined using the same threshold of the unbinding kinetics.
The lowest and highest values of the dissociation constant are in boldface.

Robustnes of affinity upon changes in DMSO concentration.

[DMSO] (mM)	τ_{on} (ns)	τ_{off} (ns)	k_{off}/k_{on} [a] (mM)	Active site occupancy %	K_D [b] (mM)
220	9.4	3.6	574	43	292
440	2.6	4.1	279	55	360
880	2.1	3.2	577	73	325

Table 2: [a]**Kinetic analysis.** Dissociation constant from fitting of cumulative distributions of unbinding and binding times. The characteristic time of the slow phase of the double-exponential fitting is used to calculate the binding rate $k_{on} = 1/(\tau_{on}[\text{DMSO}])$ and unbinding rate $k_{off} = 1/\tau_{off}$. The binding and unbinding thresholds used for the calculations are 4 Å and 8 Å, respectively.
[b]**Thermodynamic analysis.** Dissociation constant calculated from active site occupancy. The active site occupancy was determined using the same threshold of the unbinding kinetics (8 Å).

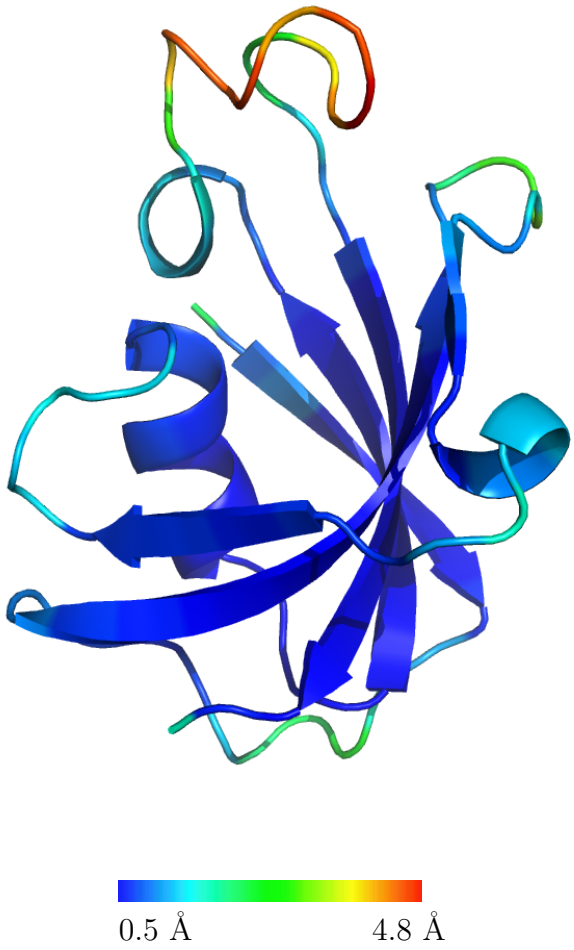

Figure 1: **Stability and flexibility of FKBP in the MD runs.** The protein is colored according to the root mean square fluctuations (RMSF) of Cα atoms. The RMSF values are calculated using the 10 MD simulations at 310 K. The coloring shows that FKBP is stable along the MD simulations, e.g., RMSF <1 Å for most of the residues. Moreover, the loop Ala84-Pro93 is the most flexible region which is consistent with the NMR spectroscopy data [10].

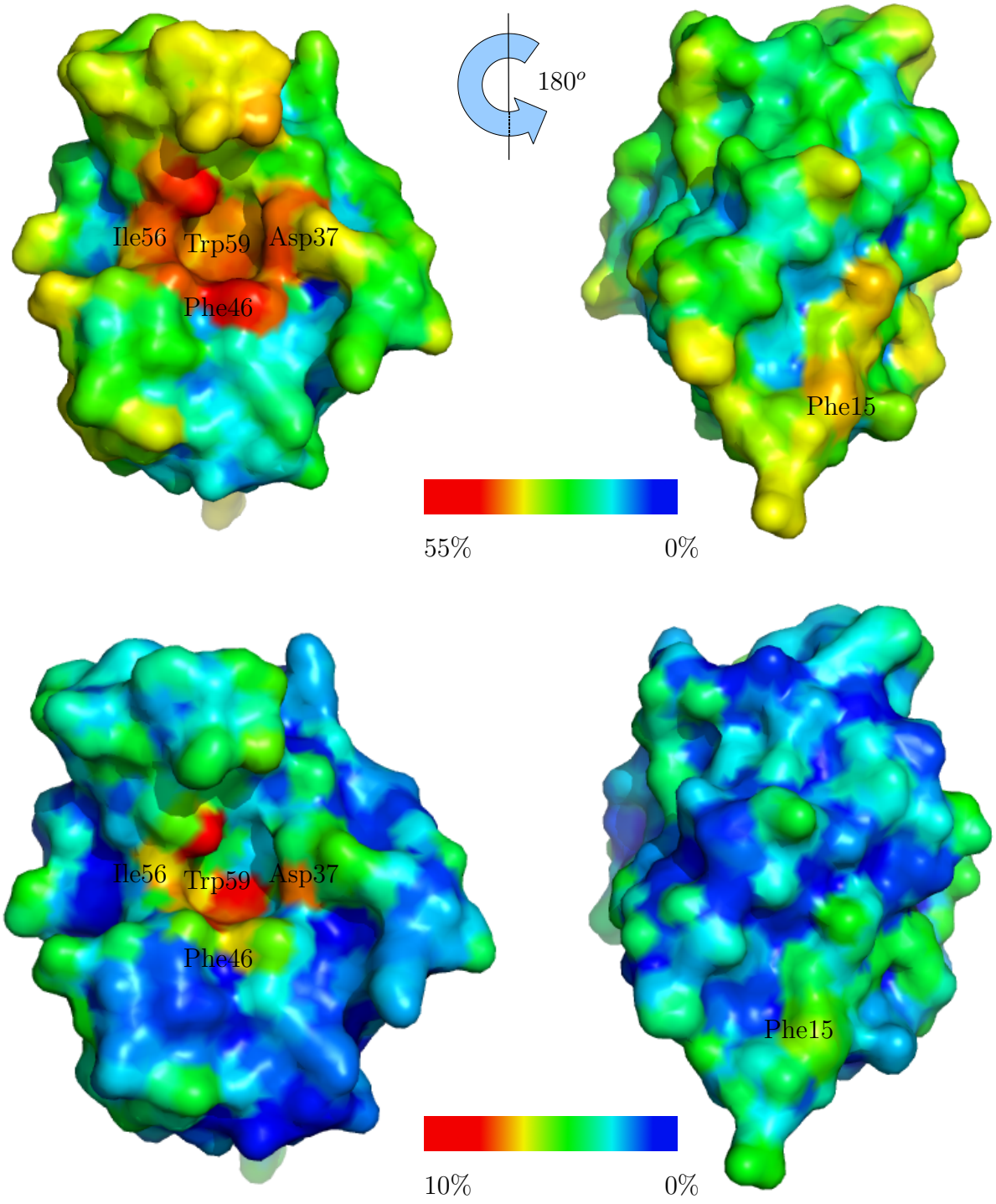

Figure 2: **Threshold dependence of the map of DMSO/FKBP contact frequencies.** Same as in Figure 1 of the main text with threshold distances of 7 Å (top) and 5 Å (bottom).

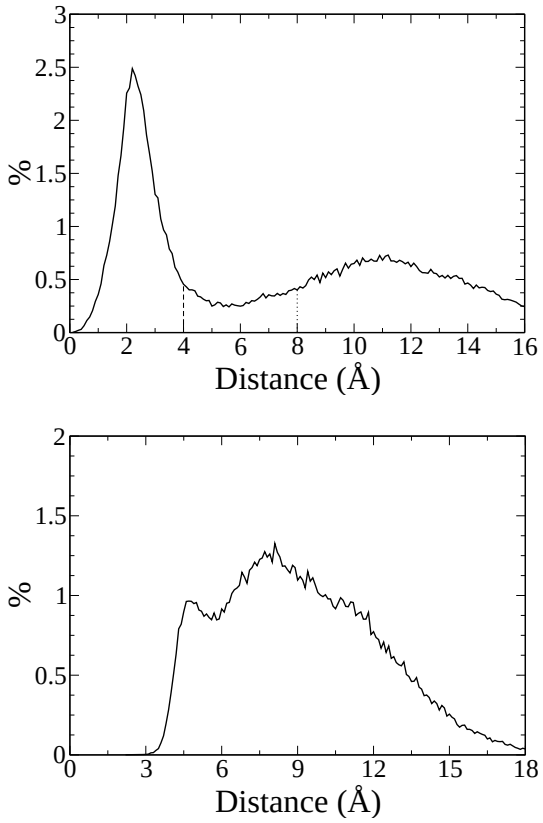

Figure 3: **Distance distributions.** (Top) Distance distribution of the DMSO molecule closest to the FKBP active site. The vertical dashed lines at 4 Å and 8 Å indicate the threshold distances used to define binding and unbinding events, respectively. (Bottom) Distance distribution of the second closest DMSO to the FKBP active site.

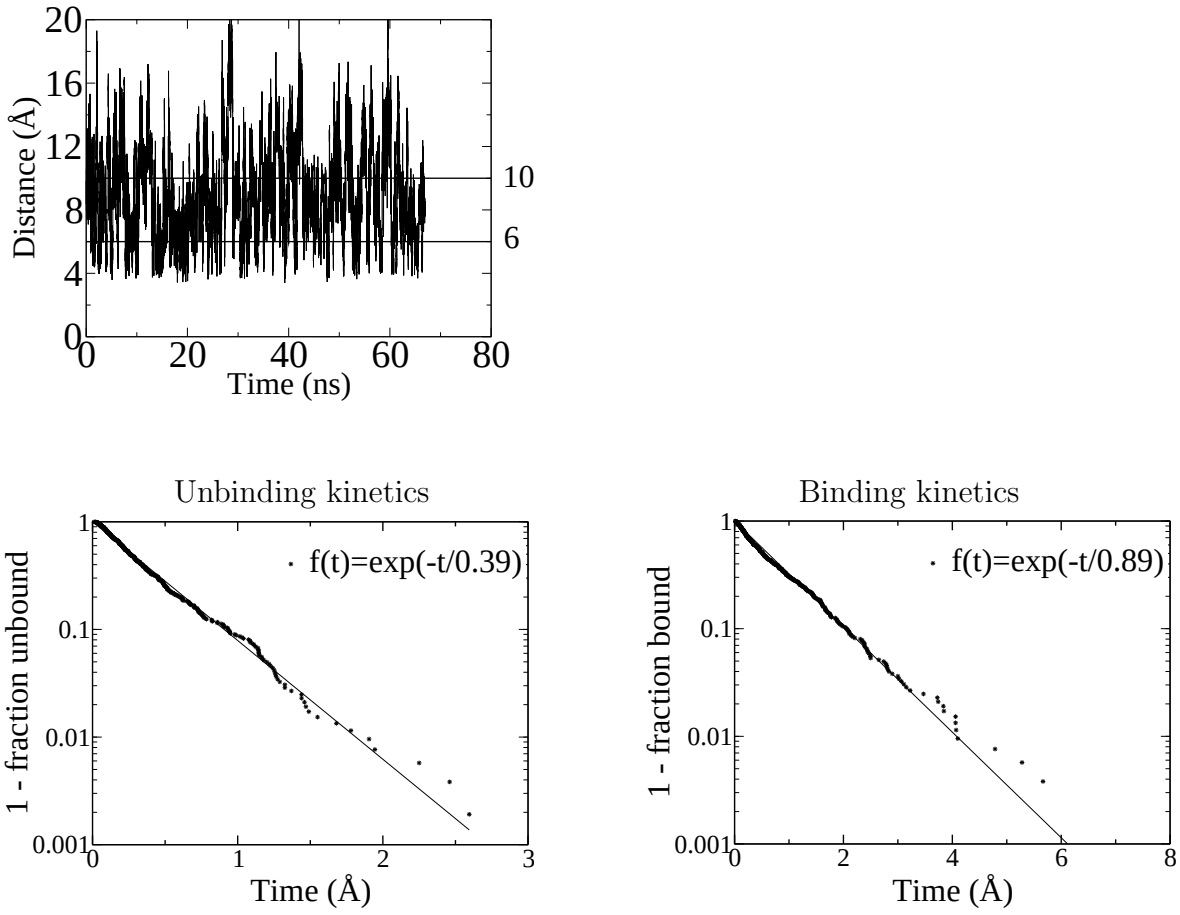

Figure 4: **Kinetics of binding to and unbinding from the minor binding site at Phe15.** (Top) Time series of the distance between centers of mass of the closest DMSO and the phenyl ring of Phe15. (Bottom) Cumulative distributions of unbinding (left) and binding (right) times from the 10 MD simulations (stars) and single-exponential fit (solid lines). Binding and unbinding events were monitored along the time series of the centers of mass distance using threshold values of 6 Å and 10 Å, respectively. These threshold values were chosen upon visual analysis of the time series, and they are shown by horizontal lines in the top panel. Note that they are larger than those used for (un)binding from/to the active site because of the different distance definitions. In other words, the concave shape of the active site yields shorter DMSO separations than the flat surface of the phenyl ring of Phe15. As an example, the distance between centers of mass of the closest DMSO and the phenyl ring of Phe15 is very sporadically shorter than 4 Å because of van der Waals repulsion. On the other hand, the distance of DMSO to the active site center (time series in Figure 2 top,right of the main text) is almost always smaller than 4 Å (in the intervals during which DMSO is bound) because of the aforementioned concave shape of the active site.